Negative refraction for incoherent atomic matter waves

Thibault Vogt[1,*] and Wenhui Li[1,2]
[1]*Centre for Quantum Technologies, National University of Singapore, Singapore 117543*
[2]*Department of Physics, National University of Singapore, Singapore 117542*
(Received 29 June 2014; published 30 March 2015)

In a recent paper [Phys. Rev. Lett. **102**, 140403 (2009)], Baudon *et al.* reported that a comoving potential acting on atoms could mimic negative-index-refraction properties of left-handed photonic metamaterials. We show in this article that a better approximation is necessary in order to describe the real physical system proposed by Baudon *et al.* We derive analytical formulas and compare their solutions with numerical simulations. It turns out that instead of negative refraction, it is simply atomic reflection that occurs in the above-mentioned comoving potential. Furthermore, we find that the wave packet of the reflected atomic beam by comoving potentials can be narrowed by negative dispersion. Finally, we identify a potential configuration, near the interface with a cubic-type potential barrier, that may lead to the observation of negative refraction with incoherent matter waves.

DOI: 10.1103/PhysRevA.91.033634 PACS number(s): 03.75.Be, 37.10.Gh, 42.25.−p

I. INTRODUCTION

Left-handed photonic metamaterials (LHMs) are materials featuring both negative electromagnetic constants ϵ and μ [1,2]. Phase and group velocities of electromagnetic planar waves propagating in such metamaterials are opposite in direction since they are determined by, respectively, the wave vector **k** and Poynting vector **S**. The refractive index is then considered negative for satisfying causality principles, i.e., $n = -(\epsilon\mu)^{1/2}$. A striking characteristic following Snell's law is that negative refraction can be observed at the interface between positive- and negative-refractive-index materials. LHMs could be used to realize perfect lenses or complete cloaking of objects from electromagnetic fields [3,4]. LHMs were first realized at the beginning of the previous decade for microwave frequencies [5]. Complete proof of their feasibility was validated with the observation of negative-index refraction [6–8]. However, it is only recently that such metamaterials have been demonstrated at visible and UV frequencies where they require a high degree of subwavelength nanostructuring [9–11]. Following the success of the development of LHMs, proposals have emerged in solid-state physics for realizing the properties of LHMs with electron waves propagating in graphene [12]. This system governed by the relativistic Dirac equation could be interesting for studying the Klein tunneling recently demonstrated in cold-atom physics [13]. Lately, in an atom optics analog, negative refraction and Veselago lensing were demonstrated for coherent matter waves propagating in an optical lattice [14].

Negative refraction in atom optics would be very valuable if it could be applied to incoherent atomic beams, which are used in many interferometric applications. The realization of Ref. [14] could hardly be extended to incoherent matter waves as it requires the wave packet to populate initially only a narrow range of quasimomenta in the ground Bloch band of an optical lattice. Recently, comoving potentials have been proposed as a promising means to mimic negative refraction for atomic beams [15]. Should such large negative refraction have been obtained, it could have led to quasiperfect focus of atomic beams or the demonstration of the propagation of atomic surface waves [16,17]. The simultaneous occurrence of negative refraction and compensation of the dispersion of wave packets resulting from the interaction with the comoving potential, typical of time reversal for atomic beams, would have been of particular interest for the realization of interferometers of great accuracy [18].

The idea of Ref. [15] was to modify the group velocity of a wave packet (of an atom) using a potential of the form

$$V(x,t) = S(t)\cos(2\pi x/\lambda),$$

where $S(t)$ stands for the time dependence of the interaction and λ is a spatial period. This type of potential could be based either on pulsed alternating magnetic fields or pulsed optical standing waves and corresponds roughly to a comoving potential[1] as some of its Fourier components are moving at a velocity v close to that of the atoms [19].

The effect of such potential, as derived in Ref. [15], was assumed to introduce a phase shift $\Delta\Phi(t,k)$ equal to

$$\Delta\Phi(t,k) = -\hbar^{-1}\int_0^t dt'\, S(t')\cos\left(2\pi\frac{\hbar k}{M\lambda}t'\right), \qquad (1)$$

where M is the mass of the atom and k a wave vector of the reciprocal Fourier space, the wave packet being initially centered around k_0. Notice here the wave packet is restricted to one dimension as in the other two directions it is not affected by the potential and follows free propagation evolution. From this expression, the group velocity along the direction of the comoving potential x was calculated as [15]

$$v_g(t,k_0) = \frac{\hbar k_0}{M} - \frac{2\pi}{M\lambda}t\, S(t)\sin\left(2\pi\frac{\hbar k_0}{M\lambda}t\right). \qquad (2)$$

[1]The Fourier transform of the potential is given by $V(x,t) = \int_{-\infty}^{\infty} d\nu\tilde{S}(\nu)e^{2i\pi\nu t}\cos(2\pi x/\lambda)$. Hence, for a real spectrum $\tilde{S}(\nu)$, this potential may be written as $V(x,t) = 2\int_0^{\infty} d\nu\tilde{S}(\nu)\cos(2\pi\nu t)\cos(2\pi x/\lambda)$, the integrand being equal to the sum of two terms $\cos[2\pi(\nu t - x/\lambda)]$ and $\cos[2\pi(\nu t + x/\lambda)]$, where the first term propagates at $v = \lambda\nu$ velocity and the second has a negligible effect on the atoms.

*cqtttv@nus.edu.sg

For a plane wave, phase velocity writes $v_\varphi = \omega/k$ where ω is the angular frequency of the wave [20]. For a Gaussian wave packet with very narrow space dispersion, it may seem natural to define phase velocity at the wave-packet-center momentum $\hbar k_0$ and energy $E = \hbar\omega_0$ of the wave-packet-center position. The issue is that any arbitrary energy reference E_0 introduces an additional term equal to $\frac{E_0}{\hbar k_0}$ that can make the definition of phase velocity unphysical. In order to lift this ambiguity, previous authors have referred directly to k_0 for describing the direction of phase propagation instead of phase velocity [14,15]. For numerical purposes, we extend this definition and take the expression of phase gradient $\partial_x\varphi(x,t)$, where $\varphi(x,t)$ is the phase of the wave function given in space representation. This phase gradient can be evaluated over the entire space and its calculation will be reviewed in Sec. III C. However, phase gradient and conjugate center momentum $\hbar k_0$ are not gauge invariant either. We will assume that the Hamiltonian of the system is expressed in the length gauge, that means it is related to the expression in Coulomb gauge via the unitary transformation $T = \exp[-\frac{i}{\hbar}\vec{d}\cdot\vec{A}_e(\vec{r},t)]$ where $\vec{A}_e$ is the applied external vector potential and $\vec{d}$ the dipole moment of an atom (for more explanations, see for example Complement AIV in Ref. [21]). This gauge is used in most nonrelativistic atom optics textbooks and is actually best suited to expressing the system in the electric and magnetic dipole approximations.[2] It also sets a clear distinction between kinetic and potential energy with kinetic term expressed simply as $p^2/2M$ where the conjugate momentum p is equal to the actual linear momentum, thus is essential in semiclassical theories for a proper definition of atomic refractive index induced by time-independent potentials. As was set implicitly in Ref. [15], we will consider finding negative-index metamedia corresponds to finding systems where phase gradient and group velocity have opposite signs assuming the length gauge has been chosen. The definition of phase propagation direction as phase gradient should be modified in another gauge in order to ensure its invariance, which simply means the effect of the gauge transformation on the wave function should be discarded in the calculation of the gradient.

In Ref. [15], while phase gradient k_0 was assumed to be unchanged for the atoms acted upon by a comoving potential, the authors found that inversion of group velocity, from $v_g(0,k_0) = \frac{\hbar k_0}{M}$ at initial time, could be observed for right choices of the different parameters $S(t)$ and λ in Eq. (2).

In this article, we demonstrate that the variation of the Fourier amplitude $|\check{\psi}(k,t)|$ of the wave function, neglected in Ref. [15], is actually important. We find that because of this variation, the center position of the wave packet $k_0(t)$ varies with time, thereby affecting the group velocity calculation but also the direction of phase propagation. In Sec. II, we review the derivation of formula (1) and point out its limitations. We then derive a more accurate analytical formula valid essentially for a shallow potential and analyze the case of deep potentials separately. In Sec. III, we compare our formula with purely numerical results. We find the problem of deep potentials relevant to negative refraction holds large similarities with atomic reflection. We then reconsider different applications related to the use of comoving potentials and show for example that wave-packet narrowing remains an interesting perspective. Finally, we devote a lot of attention to the problem of the calculation of phase velocity and consider particularly this problem near a potential barrier, where we find negative refraction may exist.

[2]The expressions of the interaction with the magnetic field are actually the same in the length and Coulomb gauges.

II. ANALYTICAL DERIVATION

In this section, we first review the calculation leading to Eq. (2) and then derive more accurate solutions of the problem of an atom in a comoving potential. The validity of our derivations will be further verified through numerical simulation presented in Sec. III A. We consider the motion of an atom in interaction with a time-dependent comoving potential acting only upon its external degrees of freedom, i.e., not coupling its internal energy levels. The comoving potential is of the form

$$V(x,t) = S(t)\cos(\kappa x),$$

where $S(t)$ is the time-dependent pulse amplitude of the potential and $\kappa = 2\pi/\lambda$. For simplification, we will keep the notations of Ref. [15] and therein.

A. Formulation of the problem

The time evolution of the atomic wave function is given by the Schrödinger equation

$$i\hbar\partial_t\Psi(x,t) = -\frac{\hbar^2}{2M}\partial_x^2\Psi(x,t) + V(x,t)\Psi(x,t). \tag{3}$$

We apply the Fourier transform with respect to x ($x \leftrightarrow k$), defined as $\check{\psi}(k,t) = \int_{-\infty}^{+\infty}\Psi(x,t)e^{-ikx}dx$ for the wave function, where $|\check{\psi}(k,0)|$ is the amplitude of the initial wave packet centered in k_0. Then, using the interaction representation $\check{\psi}(k,t) = \Gamma(k,t)e^{-i\omega_k t}$, where $\omega_k = \frac{\hbar k^2}{2M}$, Eq. (3) simplifies to (see Appendix A 1)

$$i\hbar\partial_t\Gamma(k,t) = \frac{S(t)}{2}e^{-i\frac{\hbar\kappa^2}{2M}t}\left[e^{i\frac{\hbar k\kappa}{M}t}\Gamma(k-\kappa,t) + e^{-i\frac{\hbar k\kappa}{M}t}\Gamma(k+\kappa,t)\right]. \tag{4}$$

λ is assumed to be much larger than the de Broglie wavelength, mostly true for any supersonic beam or effusive beam of thermal atoms, so that $\kappa \ll k$ for every k belonging to the momentum distribution. Consequently, the following approximation was assumed to be valid in previous works [15] (wrongly, as we will see further):

$$\Gamma(k-\kappa,t) \approx \Gamma(k+\kappa,t) \approx \Gamma(k,t). \tag{5}$$

With this assumption, the Schrödinger equation reduces to

$$i\hbar\partial_t\Gamma(k,t) \approx S(t)e^{-i\frac{\hbar\kappa^2}{2M}t}\Gamma(k,t)\cos\left(\frac{\hbar k\kappa}{M}t\right). \tag{6}$$

If the signal $S(t)$ starts at $t = 0$, after integration we get $\Gamma(k,t) = \Gamma(k,0)e^{i\Delta\Phi(k,t)}$ with a phase shift as given in Eq. (1):

$$\Delta\Phi(k,t) = \frac{-1}{\hbar}\int_0^t dt' S(t')\cos\left(\frac{\hbar k\kappa}{M}t'\right), \tag{7}$$

where the missing factor $e^{-i\frac{\hbar\kappa^2}{2M}t}$ is neglected in comparison to the fast-varying cosine term.

From expressions (6) and (7), it is clear only the phases in the wave packet are modified, hereby leaving k_0 independent of time. From the stationary phase condition discussed in Appendix A 2, result (7) leads to expression (2) of the group velocity, which can be recast in the form

$$v_g = v_g(0)\left[1 - \frac{\epsilon}{2}\omega_0 t\sin(\omega_0 t)\right], \tag{8}$$

where $v_g(0) = \frac{\hbar k_0}{M}$, $\epsilon = \frac{S}{\hbar^2 k_0^2/2M}$, and $\omega_0 = \frac{\hbar\kappa k_0}{M}$.

It is known from the first-order time-dependent complex WKB approximation [22,23] that the atoms should follow the classical trajectory in the limit of small de Broglie wavelength. Non-negligible change of kinetic energy is to be expected classically. In a quantum description $k_{0t} \equiv k_0(t)$, center wave vector of the wave packet at time t should also change. A classical calculation in the limit of small constant potential amplitude $S(t) = S(0) = S$ and large kinetic energies provides the following unambiguous result obtained in Appendix B if we assume $S(t > 0) = S$ and $S(t < 0) = 0$:

$$v_g(t) = v_g(0)\left\{1 + \frac{\epsilon}{2}[1 - \cos(\omega_0 t)]\right\}. \tag{9}$$

Although the group velocity variations in Eqs. (8) and (9) are of the same order, they behave completely differently. The velocity change in Eq. (8) alternates between positive and negative and the envelope of this velocity change goes linearly to ∞ while it is unidirectional and always given by the sign of ϵ in Eq. (9). Obviously, there must be a missing term that was forgotten in the above derivation of Eq. (8). We have actually already mentioned that approximation (5) was the problem and the reason why k_{0t} was found constant.

B. Analytical derivation

In this section, we derive the group velocity using a better approximation than the one leading to Eq. (8). The additional terms included here turn out to be essential to describe the physical system. After the derivation and discussion on the case of shallow comoving potentials, we will look into the deep potential case.

1. Derivation for shallow potentials

The comoving potential is introducing a modulation with period $2\pi/\kappa$, such that $\Gamma(k,t)$ varies on the κ scale. Therefore, approximation (5) cannot hold. As a verification, we can further expand $\Gamma(k \pm \kappa, t)$ and express it to first order:

$$\Gamma(k \pm \kappa, t) \approx \Gamma(k,t) \pm \kappa\frac{\partial\Gamma}{\partial k}. \tag{10}$$

Rewriting (4), we obtain

$$i\hbar\partial_t\Gamma \approx S(t)\left[\Gamma\cos\left(\frac{\hbar k\kappa}{M}t\right) - i\kappa\frac{\partial\Gamma}{\partial k}\sin\left(\frac{\hbar k\kappa}{M}t\right)\right]. \tag{11}$$

In this expression, we have kept the approximation $\omega_\kappa t = \frac{\hbar\kappa^2 t}{2M} \ll 1$. We further simplify the problem with the assumption of an initial Gaussian wave packet, looking for a solution ξ of the form

$$\Gamma(k,t) = \Gamma(k,0)\xi(k,t) = \frac{e^{-\frac{\Delta k^2}{2\delta k^2}}}{(\delta k^2/4\pi)^{1/4}}\xi(k,t),$$

where $\Delta k = k - k_0$.

With this initial condition and in the limit of shallow potentials, a calculation derived in Appendix A 3 yields the following expression for ξ:

$$\xi(k,t) = e^{\int_0^t dt'\omega_p(t')[-i\cos(\beta k t') + \frac{\Delta k}{\omega_{\delta k}}\beta\sin(\beta k t')]}.$$

where $\omega_p(t) = S(t)/\hbar$, $\beta = \hbar\kappa/M$ and $\omega_{\delta k} = \hbar\delta k^2/M$. This solution is valid when condition $|\omega_p|\omega_\kappa t^2 \ll 1$ is fulfilled. Considering the characteristic time $t_0 = \frac{\pi M}{\hbar\kappa k_0}$, this condition is indeed equivalent to considering a shallow potential $|\epsilon(k_0)| \ll 1$, where $\epsilon(k) = \frac{S}{\hbar^2 k^2/2M}$. Finally, Γ is given by

$$\Gamma(k,t) = \frac{e^{-\frac{\Delta k^2}{2\delta k^2}}}{(\delta k^2/4\pi)^{1/4}}e^{-i\frac{\omega_p}{\beta k}\sin(\beta k t)}e^{\frac{\omega_p}{\omega_{\delta k}}\frac{\Delta k}{k}(1-\cos(\beta k t))}, \tag{12}$$

in case $S(t > 0) = S$ and $S(t < 0) = 0$, i.e., taking ω_p constant.

2. Discussion of the result

We turn to the analysis of our solution (12), valid for shallow potentials. We must notice that for this solution, approximation (10) is indeed valid as $\kappa\partial_k\Gamma \sim \epsilon$ while $\kappa^2\partial_k^2\Gamma \sim \epsilon\kappa/k_0$ is much smaller.

The phase shift, as calculated in Ref. [15], remains given by

$$\Delta\Phi(k,t) = -\int_0^t dt'\frac{S}{\hbar}\cos(\beta k t'),$$

but there is an additional correction on the amplitude, given by the argument

$$\int_0^t dt'\frac{\omega_p}{\omega_{\delta k}}\frac{\Delta k}{k}\sin(\beta k t') = \frac{\epsilon(k)k\Delta k}{2\delta k^2}[1 - \cos(\beta k t)],$$

after integration for ω_p constant.

The new wave-packet center is a solution of

$$\partial_k\left\{-\frac{\Delta k^2}{2\delta k^2} + \frac{\epsilon(k)k\Delta k}{2\delta k^2}[1 - \cos(\beta k t)]\right\} = 0.$$

It can be evaluated easily as $\Delta k_{0t} = k_{0t} - k_0$ remains very small compared to k_0 for shallow potentials as shown in Appendix A 4:

$$k_{0t} = k_0 + \frac{\epsilon(k_0)}{2}k_0\left[1 - \cos\left(\frac{\hbar k_0\kappa t}{M}\right)\right]. \tag{13}$$

This result is equivalent to the result of Eq. (9). It simply means the atom follows the classical trajectory as derived in Appendix B in the limit of a weak interaction potential and large kinetic energy.

In case the initial position is $x_M(0) = x_0 \neq 0$, the initial expression for Γ can be approximated by

$\Gamma(k,0) = \frac{e^{-\frac{\Delta k^2}{2\delta k^2}}}{(\delta k^2/4\pi)^{1/4}} e^{-i\Delta k x_0}$. Thus, after a similar calculation[3] based on the stationary phase condition, the group velocity is found to remain equal to the result of classical mechanics obtained in Appendix B:

$$v_g(t) = v_g(0)\left\{1+\frac{\epsilon(k_0)}{2}\left[\cos\kappa x_0 - \cos\left(\frac{\hbar k_0 \kappa t}{M} + \kappa x_0\right)\right]\right\}. \tag{14}$$

Equation (A7) could be used to evaluate more accurately the new wave-packet center for deeper potentials, especially since assumption $|\omega_p|\omega_\kappa t^2 \ll 1$ should remain valid at short times even in presence of larger potentials. However, it must be reminded that the solution found this way will remain approximate as $\Gamma(k \pm \kappa, t)$ was linearized.

3. *Deep potential case*

Actually, for very deep periodic and static potential, the atom is confined near the bottom of the potential and the system is equivalent to the very well-known problem of a Gaussian wave packet inside a harmonic potential [24]. The general solution of this system is

$$\Psi(k,t) = \left(\frac{\pi}{-i\alpha_t}\right)^{1/2} e^{-i(k-k_{0t})^2/(4\alpha_t) - ikx_M + i\gamma_t}. \tag{15}$$

In this expression, $x_M = v_0/\omega \sin(\omega t)$ and $k_{0t} = Mv_0/\hbar \cos(\omega t)$ are the position center and momentum center of the wave packet, where $\omega = \kappa\sqrt{-S/M} = \sqrt{-\epsilon/2}\,\omega_0$ and where it was assumed $x_M(0) = 0$. The time-dependent width of the wave packet is given by

$$\alpha_t = -\frac{M\omega}{2\hbar}\left[\frac{\frac{1}{2}M\omega - \alpha_0\hbar\cot(\omega t)}{\alpha_0\hbar + \frac{1}{2}M\omega\cot(\omega t)}\right],$$

where $\alpha_0 = i\delta k^2/2$ and the time derivative of γ_t satisfies

$$\dot\gamma_t = i\hbar\alpha_t/M + k_{0t}\dot x_M - (S/\hbar + \omega_{k_0}).$$

If we consider $\Gamma(k,t) = \Psi(k,t)e^{i\omega_k t}$, it is clear now that approximation (10) is not valid.[4]

In conclusion, we have obtained two approximate solutions for shallow and very deep potentials. Before providing any further analysis in regard to negative refraction, a numerical simulation of the Schrödinger equation without approximation (10) will be necessary in order to solve the problem of potentials whose depth is comparable to the initial kinetic energy of the atoms.

[3]It is convenient to perform the change $\Gamma(k,t) \to \Gamma(k,t)e^{-i\Delta k x_0}$ directly in Eq. (4), hence leading to the simple replacement $\frac{\hbar k\kappa t}{M} \to \frac{\hbar k\kappa t}{M} + \kappa x_0$ in all the subsequent equations.

[4]As $\kappa\partial_k\Gamma = \kappa\Gamma[\frac{-(k-k_{0t})}{2\alpha_t} - ix_M + \frac{i\hbar k t}{M}]$, the leading term is $\frac{k\delta k^2}{2\epsilon\,\kappa k_0^2}$ for $\omega t = \pi/2$, which can be very large as $\delta_k \sim k_0$ and $-k/(\kappa\epsilon) \gg 1$. Similarly, the leading term of $\kappa^2\partial_k^2\Gamma$ scales like $\frac{k^2\delta k^4}{4\epsilon^2\,\kappa^2 k_0^4}$ for $\omega t = \pi/2$, likely to be even larger than $\kappa\partial_k\Gamma$.

III. NUMERICAL SIMULATION

In this section, we compare our analytical solutions (12) and (15) to numerical simulations, both quantum and classical. We investigate in detail the problem of negative refraction with deep potentials. We show that the solution of this system corresponds mostly to a problem of atomic reflection. We particularly review the possibility to realize time reversal with simultaneous inversion of velocity and wave-packet narrowing as was proposed initially in Ref. [18]. Eventually, a peculiar feature is found at the limit of highly dispersive atomic wave packets near a potential barrier that may lead to the observation of negative refraction.

All the results are obtained by direct computation of the temporal evolution of a wave packet interacting with a comoving potential $V(x) = S\cos(2\pi x/\lambda)$ suddenly switched on at $t = 0$. The wave packet initially fits a Gaussian

$$\Psi(x,0) = \left(\frac{1}{\pi\delta_x^2}\right)^{1/4} e^{-\frac{(x-x_0)^2}{2\delta_x^2}} e^{ik_0 x}, \tag{16}$$

where k_0 is the initial central momentum of the wave packet, $\delta k = \frac{1}{\delta_x}$ is its momentum width as defined previously. We take $x_0 = \lambda$ unless specified otherwise for the atoms to be situated at the bottom of a potential well at $t = 0$.

The evolution of the wave packet $\Psi(x,t)$ is given by the Schrödinger equation

$$i\partial_t\Psi = \frac{-\hbar}{2M}\partial_x^2\Psi + \omega_p\cos(\kappa x)\Psi, \tag{17}$$

with $\omega_p = S/\hbar$ and $\kappa = 2\pi/\lambda$. For convenience, we use reduced variables, position $u = \kappa x$ and time $\tau = \frac{\hbar\kappa^2}{2M}t = \omega_\kappa t$, replacing Eq. (17) by

$$i\partial_\tau\Psi = -\partial_u^2\Psi + \epsilon\alpha^2\cos(u)\Psi, \tag{18}$$

where we have defined the momentum ratio $\alpha = k_0/\kappa$ and potential to kinetic energy ratio $\epsilon = \omega_p/\omega_{k_0}$. The solution of this equation is obtained with the integrated IDA solver from *Mathematica*.

A. Comparison with analytical results

We compare here the numerical solution for the temporal evolution of the wave-packet-center position to the different analytical solutions derived in the previous section. The wave-packet-center position x_M is defined as the maximum of the probability density in analogy with the stationary phase approximation [20].

For free propagation of a Gaussian wave packet, the spatial center is given by $u_f(\tau) = 2\alpha\tau$. For shallow potentials, we compute numerically the difference $\Delta u_n(\tau) = \kappa x_M(\tau) - u_f(\tau)$ between the central position of the wave packet calculated with Eq. (18) and that of free propagation. The result is shown in Fig. 1. It is also compared to the following analytical value obtained after integration of the solution (13) for a potential plugged in at $t = 0$ with constant amplitude

$$\Delta u_a = \epsilon\alpha\left[\tau - \frac{\sin(2\alpha\tau)}{2\alpha}\right]. \tag{19}$$

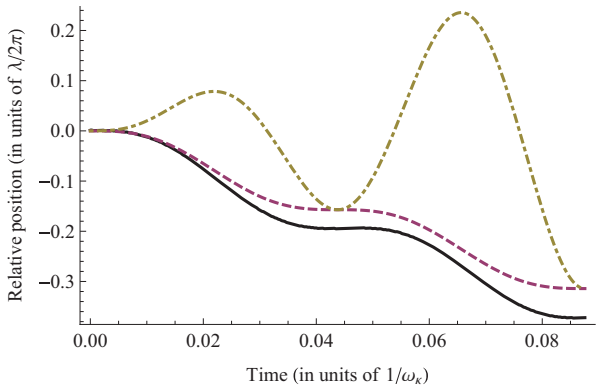

FIG. 1. (Color online) Analytical result of the relative position of the wave-packet center Δu_a from Eq. (19) (dashed curve) in comparison to the numerical result Δu_n (solid curve) and previous analytical solution from Eq. (2) (dotted-dashed curve) for $\alpha = 72$ and $\epsilon = -0.05$ (see text).

The agreement between the two is reasonably good as shown in Fig. 1 for an already large $\epsilon = -0.05$ potential. In contrast, formula (2) yields a completely erroneous result.

In order to illustrate the case of deeper potentials, corresponding to relatively large ϵ, we compare directly the numerical result of the central position of the wave packet $u_n(\tau)$ to the linear dependence $u_f(\tau) = 2\alpha\tau$ of free propagation, as shown in Fig. 2. The group velocity inversion appears quite clearly. In this figure, we also plot the result of our approximate analytical solution (13). Although accurate for short times, the latter fails to give a good estimation at large τ. This is not surprising as the motion is almost harmonic for $|\epsilon| \geqslant 2$ and is actually already better described by formula (15) for $\epsilon = -1.25$ as shown in Fig. 2 as well. The numerical curves contain a small discontinuity which is due to the appearance

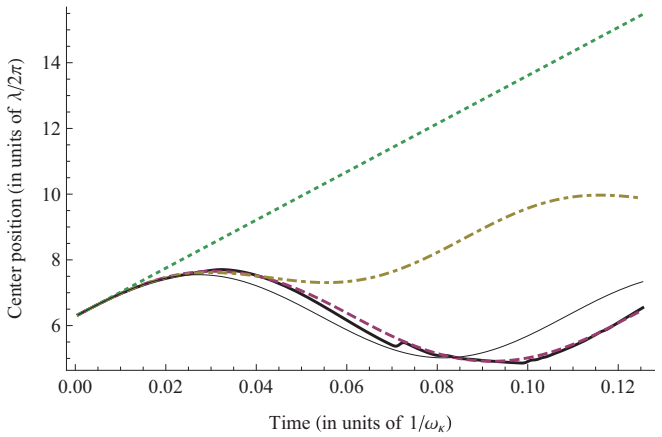

FIG. 2. (Color online) Absolute position of the wave-packet center $u(\tau)$ in units of $\lambda/2\pi$ as a function of time, calculated under different conditions: quantum numerical simulation in presence of group velocity inversion ($\epsilon = -1.25$ and $\alpha = 37$ and $\delta k = \frac{\kappa}{2\pi 0.1}$) (bold solid curve); classical numerical simulation with similar potential (dashed curve); harmonic potential approximation for deep potential (thin solid curve); shallow potential approximate result from Eq. (13) for an identical potential (dotted-dashed curve); free propagation case (dashed line).

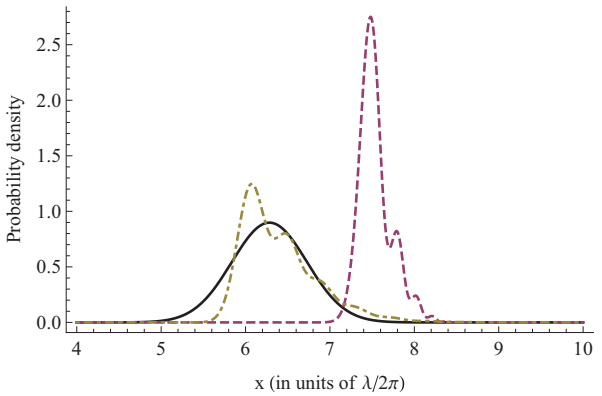

FIG. 3. (Color online) Wave packet versus position x at different times during the interaction with a periodical potential, whose parameters are the ones given in Fig. 2. (Solid line) initial wave packet with center position $x_M(0) = \lambda$; (dashed line) intermediate-time wave packet, after reflection; (dotted-dashed line) wave packet with complete inversion of the group velocity.

of slight oscillations after reflection and slight modulations of the positions of the maximum of the wave packet as shown in Fig. 3.

B. Comparison with a classical simulation

In Fig. 2, we also compare the result of the quantum simulation with the classical motion described by Newton's equations (given in Appendix B). Except for a slight effect due to wiggles in the wave packet, it is clear the quantum dynamics of the center position of the wave packet is no different than the classical dynamics of a punctual object. Such an observation is not surprising as the de Broglie wavelength used in the simulation is much smaller than the period of the potential ($\alpha = 72$). In most practical situations, α is even larger. In other words, the potential is almost constant on the scale of the wave function. As given by Ehrenfest theorem and as long as the temporal spreading of the wave packet due to dispersion is small compared to the period of the potential, the dynamics of this system is mostly classical. From a classical point of view, if a different choice is made for the initial position x_0, there can even be acceleration by the potential rather than deceleration and inversion of velocity.

In Ref. [25], it was proposed to use the same pulsed optical potential for slowing atoms by decreasing their group velocity. Although that study is somewhat disconnected from the purpose of this article, it is interesting to realize that the problem is also purely classical. Actually, slowing of atoms by pulsed standing waves is still possible according to our improved calculation and it is similar to optical Stark deceleration. A periodic potential is pulsed such that the atoms always adiabatically follow classical trajectories on the rising slopes of the potential, therefore removing their kinetic energy [26–29].

C. Is there negative refraction with comoving potentials?

In the previous subsection, we have seen that the motion of the atoms in the comoving potential remains mostly classical, which is not a good indication for the presence of negative

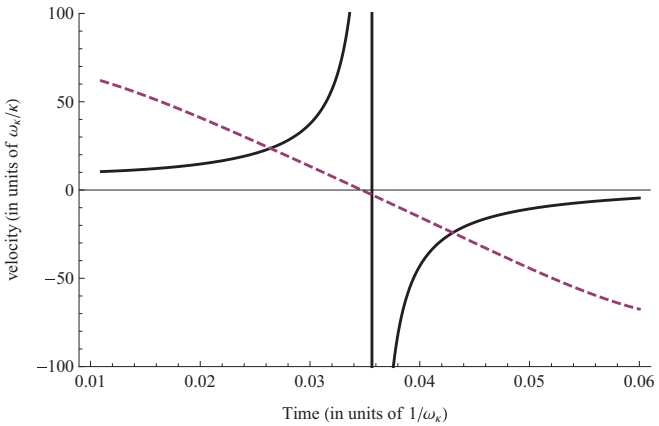

FIG. 4. (Color online) Numerical calculation of the group velocity (dashed line) and phase velocity (solid line) as a function of interacting time for a spatially narrow wave packet $\delta_x = 0.02\lambda$, with potential depth $\epsilon = -1.0$ and $\alpha = 36$. We added an arbitrary reference energy $E_0 = 300\hbar\omega_\kappa$ for the calculation of the phase velocity, which ensures phase velocity is always positive before the turning point but does not change the interpretation of the result.

refraction. Actually, we can see in Fig. 2 that group velocity inversion occurs within less than one spatial period of the potential. We claim that this inversion of group velocity is simply due to reflection of the atoms on the potential barrier and is not due to negative refraction. Starting from the bottom of a potential well with a given initial velocity, the atoms adiabatically follow the potential until they are reflected back if the potential energy barrier is larger than the initial kinetic energy. Therefore, the atoms are simply confined in one potential well. To confirm this result, we plot phase velocity versus group velocity in Fig. 4 according to the formula $v_\varphi(k_{0t},t) = -\frac{\partial_t\varphi(x_M,t)}{\partial_x\varphi(x_M,t)}$ where $\varphi(x_M,t)$ is the phase of the wave function calculated numerically. We remind here $x_M(t)$ is the center of the wave packet at time t. A divergence and inversion of phase velocity is observed at the point of group velocity inversion which is due to the fact the instantaneous phase gradient $\partial_x\varphi(x_M,t)$ cancels out and changes sign. Indeed, this behavior can be understood from Eq. (A1) for the expression of the phase $\Phi(x,k,t)$. Using this equation at first order in $k - k_{0t}$, the wave function reads as

$$\begin{aligned}\Psi(x,t) &= \frac{1}{2\pi}\int_{-\infty}^{+\infty} dk|\check{\psi}(k,t)|e^{i\Phi(x,k,t)} \\ &\approx \frac{1}{2\pi}\int_{-\infty}^{+\infty} dk|\check{\psi}(k,t)| \\ &\quad\times e^{i[(k_{0t}x-\omega_{k_{0t}}t)+\Delta\Phi(k_{0t},t)]}e^{i(k-k_{0t})[x-x_M(t)]},\end{aligned}$$

where it is assumed $\Phi(x,k,0) = kx$. We can further approximate $|\check{\psi}(k,t)|$ to be a Gaussian centered around k_{0t}, i.e., $|\check{\psi}(k,t)| = g_t(k-k_{0t})$ in analogy with the Gaussian wave-packet dynamics approximation [24]. Therefore, the wave function reads as

$$\Psi(x,t) = e^{i[(k_{0t}x-\omega_{k_{0t}}t)+\Delta\Phi(k_{0t},t)]}\check{g}_t[x - x_M(t)], \qquad (20)$$

with total phase $\varphi(x,t) = k_{0t}x - \omega_{k_{0t}}t + \Delta\Phi(k_{0t},t)$. This expression for the wave packet shows very clearly how an instantaneous phase gradient can be defined as $\partial_x\varphi(x,t) \approx k_{0t}$ while the instantaneous angular frequency is $-\partial_t\varphi(x,t)$. Instantaneous phase velocity is obviously given by

$$v_\varphi(k_{0t},t) = -\frac{\partial_t\varphi(x,t)}{\partial_x\varphi(x,t)} = \frac{\hbar k_{0t}}{2M} - \frac{\partial_t\Delta\Phi(k_{0t},t)}{k_{0t}},$$

which diverges and changes sign at the turning point, an effect well known from semiclassical theories [30]. The quasi simultaneous change of sign for phase gradient and group velocity is actually the result that constitutes a seminal feature of reflection. As explained in introduction, phase velocity systematically diverges to $+\infty$ before the turning point and $-\infty$ after the turning point only if a sufficiently large energy reference is added to the Hamiltonian such that $-\partial_t\varphi(x,t)$ is large and positive. Those results are of course quite similar for time dependent potentials with slowly decreasing amplitudes such as considered in Ref. [15].

In conclusion, we find no indication of negative refraction but rather indications of atomic reflection, that can mimic certain results of optical negative refraction but shall not be confused with them.

D. Wave-packet spatial narrowing

We have shown that group velocity inversion is not caused by negative refraction but due to atomic reflection. Here, we investigate an important application of the initially proposed negative-refraction method, namely, simultaneous occurrence of group velocity inversion and compensation of wave-packet dispersion, which could have interesting application in interferometry [18]. When comparing the wave packet after full reflection to the initial one, a decreasing of its spatial dispersion can be seen (cf. Fig. 3). Here, the dispersion is defined as the full width at half maximum (FWHM) of the probability distribution of the wave packet. This dispersion shrinking can be somewhat interpreted if we try to provide a more accurate expression for the wave function (20) by using the development (A1) of the phase $\Phi(x,k,t)$ at second order around k_{0t}.

Developing the phase $\Phi(x,k,t)$ at second order around k_{0t}, the wave function reads as [20]

$$\begin{aligned}\Psi(x,t) &= \frac{e^{i[k_{0t}x-\omega_{k_{0t}}t+\Delta\Phi(k_{0t},t)]}}{2\pi}\int_{-\infty}^{+\infty} g_t(k)e^{ik(x-x_M)}e^{i\frac{k^2\beta}{2}}dk \\ &= e^{i[k_{0t}x-\omega_{k_{0t}}t+\Delta\Phi(k_{0t},t)]}\frac{\left(\frac{2a^2}{\pi}\right)^{1/4}e^{i\frac{\phi_t}{2}}e^{-\frac{[x-x_M(t)]^2}{a^2-2i\beta}}}{(a^4+4\beta^2)^{1/4}}, \qquad (21)\end{aligned}$$

with $\beta(t) = \partial_k^2\Delta\Phi(k_{0t}) - \frac{\hbar t}{M}$, $\phi_t(t) = \arctan(\frac{2\beta}{a^2})$, and $a(t)^2 = \frac{2}{\delta k^2(t)}$ for a Gaussian $g_t(k)$ of width $\delta k(t)$. This expression shows the natural wave-packet spreading can be canceled by large $\partial_k^2\Delta\Phi(k_{0t})$.

However, more than free propagation expansion cancellation, numerical simulation shows spatial narrowing of the wave packet, with a final wave packet narrower than the initial one, mostly for $\delta k < 2\kappa$. Not only does the wave packet focus near the turning point, but also the spatial distribution never returns back to its initial value after full reflection, remaining narrower. In Fig. 3, we have purposely chosen potentials deep in comparison to the initial kinetic energy

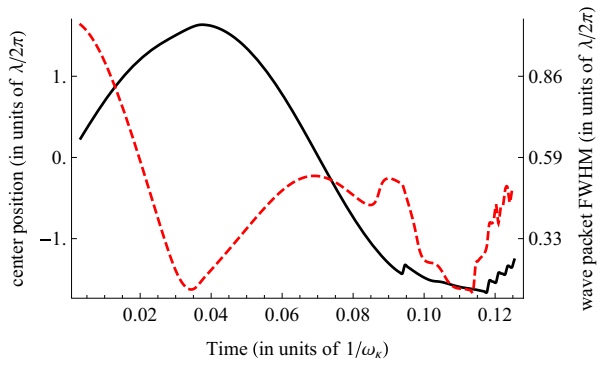

FIG. 5. (Color online) Center position of the wave packet with respect to its initial position (solid line) and wave-packet dispersion (dashed line). Parameters of the simulation are the ones of Fig. 2, except $\epsilon = -1.0$ and $x_0 = 0$. Maximum inverted velocity (slope of the center position curve) is reached at $t \sim 0.07/\omega_\kappa$. Large wiggles appear for $t > 0.08/\omega_\kappa$.

to emphasize the wiggles effect, but shallower potentials, down to the $\epsilon/2$ threshold for reflection, produce more regular trajectories and less deformation of the wave packet. Actually, there seems to exist a best potential for dispersion narrowing for our choice of parameters, situated around $\epsilon = -1.0$, with up to 50% narrowing when inverted velocity is maximum as shown in Fig. 5. This decreasing in wave-packet width seems also to increase with α but is only valid for initially largely spread wave packets. The width taken so far, $\delta_x = 0.1\lambda$, corresponds to a momentum width $\delta k = \delta_x^{-1}$ and a temperature $T = \frac{\hbar^2 \delta k^2}{6 M k_B} \sim 0.6\ \mu$K of a rubidium thermal gas if the potential has a period $\lambda = 0.4\ \mu$m. Narrowing can become more pronounced at lower temperatures, to the expense of larger wiggles. Wave-packet narrowing disappears rapidly at larger temperatures where it is even replaced by dispersion. Indeed, for large-momentum distribution, natural dispersion cannot be canceled by negative dispersion from the potential and the wave packet does not focus around the turning point.

E. Negative refraction at a cubic potential barrier

Wave-packet narrowing cannot be explained at second-order expansion of the phase $\Phi(x,k,t)$ assuming a Gaussian wave packet. Hence, it is a result that cannot be described by the Gaussian wave-packet dynamics approximation [24] and must be due to the nonharmonic terms in the potential. Similarly, there is a very slight delay in Fig. 4 between the times when phase and group velocities change sign, that cannot be accounted for with the Gaussian approximation of the wave function either. Indeed, expression (21) would yield the following phase for the wave function:

$$\varphi(x,t) = k_{0t}x - \omega_{k_{0t}}t + \Delta\Phi(k_{0t},t) - \frac{\arctan\left(\frac{2\beta}{a^2}\right)}{2} + \frac{2\beta(x - x_M)^2}{a^4 + 4\beta^2},$$

and the following expression for the phase gradient

$$\partial_x\varphi(x,t) = k_{0t} + \frac{4\beta(x - x_M)}{a^4 + 4\beta^2}.$$

The phase gradient is calculated at $x(t) = x_M(t)$ in the expression of the phase velocity in Fig. 4. Thus, it would be simply equal to k_{0t} and cancel out exactly for $k_{0t} = 0$. That would mean a divergence and change of the sign of phase velocity for $k_{0t} = 0$. Since $k_{0t} = 0$ is defined as the turning point where group velocity also changes sign, no delay would be seen in Fig. 4.

This velocity lag has to do with the non-Gaussian spreading of the wave packet and the rapid evolution of the phase at the turning point. While the position of the wave packet is almost stationary around the turning point, the phase is changing very rapidly. The velocity delay appears only for $\delta k > 10\kappa$, and can become very large for wave packets with larger-momentum distribution. Thus, in theory, as defined here, negative refraction occurs during this short delay before full reflection of the wave packet.

To be more quantitative, we examine the effect of the anharmonic terms of the $V(u) = \epsilon \cos u$ potential where we remind $u = \kappa x$, taken for $\epsilon \sim -1$ at which value the effects we observe happen. With such a potential, reflection occurs when $u \sim \pi/2$, that means the potential is well approximated as $V(u) = -[(\pi/2 - u) - \frac{(\pi/2-u)^3}{3!}]$ around reflection. To analyze the role of the anharmonic cubic term, we simulate the effect of a cubic potential barrier, with a potential of the form

$$V(u) = N[(\pi/2 - u) + a_3(\pi/2 - u)^3],$$

where N is adjusted such that $V(0) = -1$ at $u = 0$ where the wave packet is initially positioned. We take $\alpha = 37$ as in Figs. 2–6. We confirm that the velocity lag depends only on the presence of coefficient a_3. Interestingly, we find the group velocity changes sign before the phase gradient $\partial_x\varphi(x_M)$ does for $a_3 < 0$, but after $\partial_x\varphi(x_M)$ does for $a_3 > 0$. In Fig. 6, the velocity lag for $a_3 = \frac{1}{6}$ appears very large. Corresponding probability densities and phases of the wave packets just before phase gradient inversion and just before group velocity

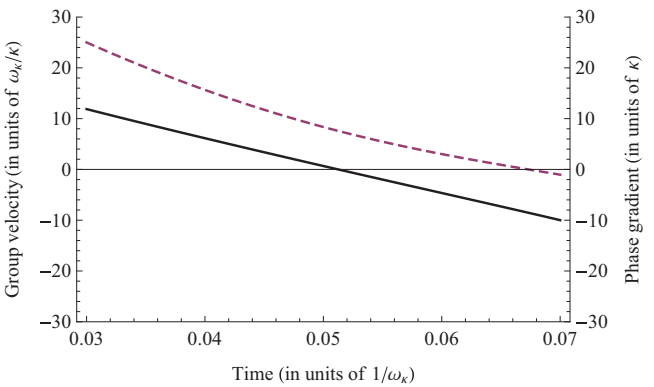

FIG. 6. (Color online) Numerical calculation of the group velocity (dashed line) and phase gradient at wave-packet center (solid line) as a function of interacting time for a spatially narrow wave packet $\delta_x = 0.02\lambda$ launched onto a cubic-type potential barrier $V(x) \propto x + a_3x^3$ where $a_3 = \frac{1}{6}$ (see text).

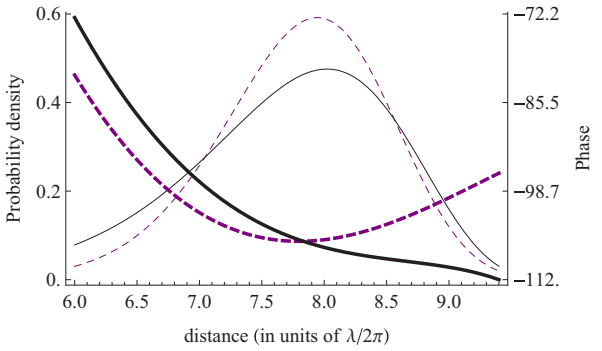

FIG. 7. (Color online) Probability densities (thin curves) and phases (bold curves) of the wave packets just before phase gradient inversion at $t = 0.048\omega_\kappa^{-1}$ (dashed curves) and close to group velocity inversion at $t = 0.06\omega_\kappa^{-1}$ (solid curves), with computation parameters as given in Fig. 6.

inversion are displayed on Fig. 7. Phase gradient is fully negative for $t = 0.06\omega_\kappa^{-1}$ while group velocity is still positive, however, at the expense of a non-Gaussian spreading of the wave packet. The behavior of the wave packet is fairly different depending upon the sign of a_3. It looks like a repulsion by the potential for $a_3 < 0$ with some slight refocusing effect at the turning point while the wave packet senses deeply into the potential barrier for $a_3 > 0$. This result clearly shows that it is possible to obtain opposite sign for phase gradient and group velocity in the vicinity of the classical turning point, hence negative refraction.

Since we are dealing with individual wave packets of rather narrow spatial dimensions, we can infer that our description is mostly valid for incoherent matter waves. We have not performed a full statistical treatment as it is beyond the scope of our paper. However, we have checked that negative refraction occurs for a large range of initial kinetic energies around $E_{\text{kin0}} = V(\pi/2) - V(0)$, from $0.8E_{\text{kin0}}$ to $1.2E_{\text{kin0}}$ namely. Therefore, it would be satisfying for incoherent matter waves with a broad statistical distribution of velocities. Practically, assuming a characteristic length $\lambda = 0.4$ μm for the potential and an initial mean velocity of the atoms launched on the barrier equal to $v_0 = 0.42$ m/s as in Fig. 4, the wave packets would have a velocity width of 0.064 m/s and a spatial extent of 8 nm and would correspond to a temperature $T = 14$ μK for a thermal gas. An optical dipole potential of a few tens of μK would be suitable for this type of experiment. The barrier potential may not be directly created but may be approximated by slightly modifying an oscillating potential. We have presented the results in reduced units which means a much wider range of parameters is accessible. However, increasing initial kinetic energy means also the potential height has to be increased. Discussing the realization of this experiment may be too premature at this point as the conditions of observation of negative refraction have not been checked yet. Especially, we have not tested whether or not this type of negative refraction can be used effectively to realize perfect focusing. One could imagine a moving potential barrier that may ensure a negative refraction occurring for a sufficiently long time to be observable.

IV. CONCLUSION

In conclusion, we find group velocity inversion in presence of comoving potential is related to reflection. Negative refraction is possible only in the vicinity of the turning point and is not limited to comoving potentials. As expected, we have shown that our perturbation analysis matches classical trajectories in the limit of small de Broglie wavelengths. A quantum simulation of the system in interaction with a large potential confirms the possibility for compensation of spatial dispersion of a wave packet at low temperature, which may be promising for interferometric application. A semiclassical complex time-dependent Wentzel-Kramers-Brillouin (CWKB) method [22,23] may also be able to capture most of the present results for larger potentials relevant to group velocity inversion and wave packet narrowing. It could be interesting in a further study to introduce the formalism of Bloch states in an optical lattice in the limit of large potentials [31,32]. It could be also interesting to go further on the analysis of cubic-type potential barrier, possibly moving, using the formalism developed for anharmonic potentials [33].

ACKNOWLEDGMENTS

We warmly thank M. Kiffner for providing us with the numerical code for the resolution of the Schrödinger equation and J. Baudon, M. Ducloy, F. Perales, and G. Dutier for thorough discussions on their related manuscripts. This work is supported by the National Research Foundation and the Ministry of Education of Singapore.

APPENDIX A: DETAILED ANALYTICAL DERIVATIONS

1. Schrödinger equation in Fourier space

This paragraph details the derivation of Eq. (4). The time evolution of the atomic wave function is given by the Schrödinger equation

$$i\hbar\partial_t\Psi(x,t) = -\frac{\hbar^2}{2M}\partial_x^2\Psi(x,t) + V(x,t)\Psi(x,t).$$

Applying the Fourier transform with respect to x ($x \leftrightarrow k$), defined as $\check{\psi}(k,t) = \int_{-\infty}^{+\infty}\Psi(x,t)e^{-ikx}dx$ where $|\check{\psi}(k,0)|$ is the amplitude of the initial wave packet centered in k_0, the equation reads as

$$i\hbar\partial_t\check{\psi}(k,t) = \omega_k\check{\psi}(k,t) + \frac{1}{2\pi}(W * \check{\psi})(k,t),$$

noting $\omega_k = \frac{\hbar k^2}{2M}$ and having written the Fourier transform of the comoving potential as

$$W(k,t) = \int_{-\infty}^{+\infty} V(x,t)e^{-ikx}dx = \pi S(t)[\delta(k-\kappa)+\delta(k+\kappa)].$$

Then, defining $\check{\psi}(k,t) = \Gamma(k,t)e^{-i\omega_k t}$, the equation simplifies to

$$i\hbar\partial_t\Gamma = \frac{1}{2\pi}e^{i\omega_k t}(W * e^{-i\omega_k t}\Gamma).$$

Therefore, we obtain

$$i\hbar\partial_t\Gamma(k,t) = \frac{S(t)}{2}e^{-i\frac{\hbar\kappa^2}{2M}t}\left[e^{i\frac{\hbar k\kappa}{M}t}\Gamma(k-\kappa,t) + e^{-i\frac{\hbar k\kappa}{M}t}\Gamma(k+\kappa,t)\right].$$

2. Stationary phase condition

The stationary phase condition states that $|\Psi(x,t)|$ is maximum in $x = x_M$ if the phase $\Phi(x,k,t)$ in the integrand of the inverse Fourier transform $\Psi(x,t) = \frac{1}{2\pi}\int_{-\infty}^{+\infty} dk|\breve{\psi}(k,t)|e^{i\Phi(x,k,t)}$ cancels out at first order around the central momentum for $x = x_M$.

The total phase in the integrand is given by

$$\Phi(x,k,t) = \Phi_0(k,0) + kx - \frac{\hbar k^2}{2M}t + \Delta\Phi(k,t),$$

where $\Phi_0(k,0)$ is the phase at $t = 0$. In order to calculate $x_M(t)$ and the group velocity $\frac{dx_M}{dt}$, the phase can be expanded around $k_{0t} \equiv k_0(t)$, center of the wave packet at time t, in the form

$$\begin{aligned}\Phi(x,k,t)&\\ &\approx \Phi_0(k_{0t},0) + \Delta\Phi(k_{0t},t) - \frac{\hbar k_{0t}^2}{2M}t + k_{0t}x\\ &\quad + (k-k_{0t})\left[\partial_k\left(\Phi_0(k,0)+\Delta\Phi(k,t)\right)|_{k_{0t}} - \frac{\hbar k_{0t}}{M}t + x\right]\\ &\quad + \frac{(k-k_{0t})^2}{2}\left\{\partial_k^2\left[\Phi_0(k,0)+\Delta\Phi(k,t)\right]|_{k_{0t}} - \frac{\hbar}{M}t\right\}.\end{aligned} \tag{A1}$$

The stationary phase condition results in

$$x_M(t) = \frac{\hbar k_{0t}}{M}t - \partial_k\left[\Phi_0(k,0)+\Delta\Phi(k,t)\right]|_{k_{0t}}.$$

The group velocity is then given by

$$v_g(t) = \frac{dx_M}{dt} = \frac{\hbar k_{0t}}{M} + \frac{\hbar}{M}\frac{dk_{0t}}{dt}t - \partial_t\partial_k\Delta\Phi(k,t)|_{k_{0t}}. \tag{A2}$$

3. Wave packet in a shallow periodical potential

It is the purpose of this paragraph to give a solution of the following equation in the limit of shallow potentials and for an initial Gaussian wave packet:

$$i\hbar\partial_t\Gamma = S(t)\left[\Gamma\cos\left(\frac{\hbar k\kappa}{M}t\right) - i\kappa\frac{\partial\Gamma}{\partial k}\sin\left(\frac{\hbar k\kappa}{M}t\right)\right]. \tag{A3}$$

Looking for a solution ξ of the form $\Gamma(k,t) = \frac{e^{-\frac{\Delta k^2}{2\delta k^2}}}{(\delta k^2/4\pi)^{1/4}}\xi(k,t)$, Eq. (A3) writes

$$\frac{\partial_t\xi}{\omega_p} = \left[\frac{\beta\Delta k}{\omega_{\delta k}}\sin(\beta kt) - i\cos(\beta kt)\right]\xi - \kappa\sin(\beta kt)\,\partial_k\xi, \tag{A4}$$

where $\omega_p(t) = S(t)/\hbar$, $\beta = \hbar\kappa/M$, and $\omega_{\delta k} = \hbar\delta k^2/M$.

We may neglect the last term in this equation. To analyze at what condition this approximation is valid, we apply the change of variables $t' = t$ and $u = \beta kt$ that implies $\partial_k\xi = \partial_u\xi\beta t'$ and $\partial_t\xi = \partial_{t'}\xi + \frac{u}{t'}\partial_u\xi$, from which we obtain

$$\partial_{t'}\xi + \frac{u}{t'}\partial_u\xi = \omega_p\left(\frac{\Delta u}{\omega_{\delta k}t'}\sin u - i\cos u\right)\xi - \omega_p\kappa\beta t'\sin u\;\partial_u\xi,$$

where we have defined $\Delta u(t') = \beta\Delta kt'$. The above equation can be recast in the form (defining $t = t'$)

$$\begin{aligned}t\partial_t\xi + u\partial_u\xi = &\left(\frac{\omega_p}{\omega_{\delta k}}\Delta u\sin u - i\omega_p t\cos u\right)\xi\\ &- 2\omega_p\omega_\kappa t^2\sin u\;\partial_u\xi.\end{aligned} \tag{A5}$$

Since $\omega_\kappa t \ll 1$, it seems natural to neglect $\omega_p\omega_\kappa t^2\sin u\partial_u\xi$ in Eq. (A5). Then, remarking that neglecting $\omega_p\omega_\kappa t^2\sin u\partial_u\xi$ in Eq. (A5) is absolutely equivalent to neglecting $\omega_p\kappa\sin(\beta kt)\partial_k\xi$ in Eq. (A4), we obtain

$$\xi(k,t) = e^{\int_0^t dt'\omega_p(t')\left[-i\cos(\beta kt') + \frac{\Delta k}{\omega_{\delta k}}\beta\sin(\beta kt')\right]},$$

in the limit of shallow potentials, which yields for Γ, in case $S(t>0) = S$ and $S(t<0) = 0$, i.e., taking ω_p constant

$$\Gamma(k,t) = \frac{e^{-\frac{\Delta k^2}{2\delta k^2}}}{(\delta k^2/4\pi)^{1/4}}e^{-i\omega_p\frac{M}{\hbar k\kappa}\sin(\frac{\hbar k\kappa}{M}t)}e^{\frac{\omega_p}{\omega_{\delta k}}\frac{\Delta k}{k}[1-\cos(\frac{\hbar k\kappa}{M}t)]}. \tag{A6}$$

If we refer to $t_0 = \frac{\pi M}{\hbar\kappa k_0} \sim \frac{2M}{\hbar k_0\kappa} = (\omega_{k_0}\omega_\kappa)^{-1/2}$ as a characteristic time in Eq. (A5), we find

$$|\omega_p|\omega_\kappa t_0^2 \ll 1 \Leftrightarrow \frac{|\omega_p|}{\omega_{k_0}} \ll 1 \Leftrightarrow |\epsilon(k_0)| \ll 1,$$

where $\epsilon(k) = \frac{S}{\hbar^2k^2/2M}$. In other words, the approximation performed in Eq. (A5) gives an analytical solution valid for potentials shallow in comparison to the initial kinetic energy of the atom. The neglected quadratic term in time from Eq. (A5) has a rather small influence at the beginning whatever the potential but one can expect its importance to increase rapidly over time for deep potentials.

4. New wave-packet center

The new wave-packet center in the limit of shallow potentials is solution of

$$\partial_k\left\{-\frac{\Delta k^2}{2\delta k^2} + \frac{\epsilon(k)k\Delta k}{2\delta k^2}\left[1-\cos(\beta kt)\right]\right\} = 0.$$

With the property $\partial_k[\epsilon(k)k\Delta k] = \epsilon(k)k_0$, the new wave-packet center fulfills the following equation:

$$\Delta k - \epsilon(k)k_0\sin^2(\beta kt/2) + \epsilon(k)\Delta k\sin(\beta kt) = 0. \tag{A7}$$

Since $\epsilon \ll 1$ and $\beta kt \sim \pi$ for $t = t_0$, it is obvious from the above equation that its solution $\Delta k_{0t} = k_{0t} - k_0$ remains very small compared to k_0. Hence, the third term of this equation can be neglected and we shall replace k by k_0 in the second term in order to calculate Δk_{0t} at first order, leading to the following simple result:

$$k_{0t} = k_0 + \frac{\epsilon(k_0)}{2}k_0\left[1-\cos\left(\frac{\hbar k_0\kappa t}{M}\right)\right],$$

where we remind k_0 stands for $k_0 = k_0(0)$.

Consequently, the expression for the group velocity is given by

$$\begin{aligned} v_g(x,t) &= \frac{\hbar k_{0t}}{M} + \frac{\hbar}{M}\frac{d\Delta k_{0t}}{dt}t - \partial_t\partial_k \Delta\Phi(k,t)|_{k_{0t}} \\ &= \frac{\hbar k_{0t}}{M} + \frac{\epsilon(k_0)}{2}k_0\frac{\hbar k_0 \kappa t}{M}\sin\left(\frac{\hbar k_0 \kappa t}{M}\right) \\ &\quad -\frac{\epsilon(k_{0t})}{2}k_{0t}\frac{\hbar k_{0t}\kappa t}{M}\sin\left(\frac{\hbar k_{0t}\kappa t}{M}\right) \\ &\approx \frac{\hbar k_{0t}}{M}, \end{aligned} \tag{A8}$$

valid in the limit of small Δk_{0t}.

APPENDIX B: CLASSICAL TRAJECTORY

1. Time-independent case

Let us first consider an atom in a potential $V(x) = S\cos(\kappa x)$, considered as a small interaction perturbation, suddenly switched on at $t = 0$. From Newton's law and conservation of total energy E_0, we can write

$$M\frac{d^2x}{dt^2} = S\kappa\sin(\kappa x) \tag{B1}$$

and

$$\frac{dx}{dt} = \sqrt{\frac{2}{M}[E_0 - S\cos(\kappa x)]}, \tag{B2}$$

with $E_0 = \frac{Mv_0^2}{2} + S\cos(\kappa x_0)$ where x_0 and v_0 are the initial conditions given from the sudden approximation.

Considering our case $|S| \ll E_0$, it must be possible to simply replace x by $x = x_0 + v_0 t$ in Eq. (B2) as the change of velocity is small. This result can easily be verified. With the assumption $|S| \ll E_0$, Eq. (B2) simplifies to

$$\begin{aligned} \frac{dx}{dt} &= \sqrt{v_0^2\left\{1 - \frac{S}{E_0}[\cos(\kappa x) - \cos(\kappa x_0)]\right\}} \\ &\approx v_0\left\{1 - \frac{\epsilon}{2}[\cos(\kappa x) - \cos(\kappa x_0)]\right\} \\ &\approx v_0\left[1 - \frac{\epsilon}{2}\cos(\kappa x)\right]\left[1 + \frac{\epsilon}{2}\cos(\kappa x_0)\right], \end{aligned}$$

with small $\epsilon = S/E_0$. We write $v_0' = v_0[1 + \frac{\epsilon}{2}\cos(\kappa x_0)]$.

The above differential equation is simply solved:

$$\begin{aligned} & dx\left[1 + \frac{\epsilon}{2}\cos(\kappa x)\right] = v_0' dt, \\ & \Leftrightarrow\ x + \frac{\epsilon}{2}\sin(\kappa x)/\kappa = v_0' t + cte, \\ & \Rightarrow\ x + \frac{M}{2E_0\kappa^2}\frac{d^2x}{dt^2} = v_0' t + cte, \\ & \Leftrightarrow\ x(t) = v_0' t + A\sin(\omega_0 t + \varphi) + cte, \end{aligned}$$

where $\omega_0 = v_0\kappa$.

Solving for the different initial conditions yields

$$x(t) = v_0' t - \frac{\epsilon v_0}{2\omega_0}[\sin(\omega_0 t + \kappa x_0) - \sin(\kappa x_0)] + x_0.$$

Eventually, we have got

$$v_g = v_0\left\{1 + \frac{\epsilon}{2}[\cos(\kappa x_0) - \cos(\omega_0 t + \kappa x_0)]\right\}$$

for the group velocity inside the potential. For $x_0 = 0$, the above expression writes

$$v_g(t) = v_g(0)\left\{1 + \frac{\epsilon}{2}[1 - \cos(\omega_0 t)]\right\}.$$

2. Numerical simulation

Equations (B1) and (B2), valid also for time-dependent potentials, can be recast in reduced units as

$$\frac{d^2u}{d\tau^2} = 2\epsilon\alpha^2\sin u \tag{B3}$$

and

$$\frac{du}{d\tau} = 2\alpha\sqrt{1 + \epsilon(\cos u_0 - \cos u)}, \tag{B4}$$

where $u = \kappa x$, $\tau = \omega_\kappa t$ knowing $\omega_\kappa = \hbar\kappa^2/2M$, $\epsilon(t) = S(t)/(Mv_0^2/2)$, and $\alpha = k_0/\kappa$. Solving numerically Eq. (B3) with initial condition $u(0) = \kappa x_0$ and $u'(0) = 2\alpha$ is straightforward.

[1] V. G. Veselago, Fiz. Tverd. Tela (Leningrad) **8**, 3571 (1966) [Sov. Phys. Solid State **8**, 2854 (1967)].

[2] D. R. Smith and N. Kroll, Phys. Rev. Lett. **85**, 2933 (2000).

[3] J. B. Pendry, Phys. Rev. Lett. **85**, 3966 (2000).

[4] J. B. Pendry, D. Schurig, and D. R. Smith, Science **312**, 1780 (2006).

[5] D. R. Smith, W. J. Padilla, D. C. Vier, S. C. Nemat-Nasser, and S. Schultz, Phys. Rev. Lett. **84**, 4184 (2000).

[6] A. A. Houck, J. B. Brock, and I. L. Chuang, Phys. Rev. Lett. **90**, 137401 (2003).

[7] C. G. Parazzoli, R. B. Greegor, K. Li, B. E. C. Koltenbah, and M. Tanielian, Phys. Rev. Lett. **90**, 107401 (2003).

[8] J. B. Pendry, Nature (London) **423**, 22 (2003).

[9] H. J. Lezec, J. A. Dionne, and H. A. Atwater, Science **316**, 430 (2007).

[10] J. Valentine, S. Zhang, T. Zentgraf, E. Ulin-Avila, D. A. Genov, G. Bartal, and X. Zhang, Nature (London) **455**, 376 (2008).

[11] T. Xu, A. Agrawal, M. Abashin, K. J. Chau, and H. J. Lezec, Nature (London) **497**, 470 (2013).

[12] V. V. Cheianov, V. Fal'ko, and B. L. Altshuler, Science **315**, 1252 (2007).

[13] V. V. Klimov, J. Baudon, and M. Ducloy, Europhys. Lett. **94**, 20006 (2011).
[14] M. Leder, C. Grossert, and M. Weitz, Nat. Commun. **5**, 3327 (2014).
[15] J. Baudon, M. Hamamda, J. Grucker, M. Boustimi, F. Perales, G. Dutier, and M. Ducloy, Phys. Rev. Lett. **102**, 140403 (2009).
[16] M. Hamamda, V. Bocvarski, F. Perales, J. Baudon, G. Dutier, C. Mainos, M. Boustimi, and M. Ducloy, J. Phys. B: At., Mol. Opt. Phys. **43**, 215301 (2010).
[17] T. Taillandier-Loize, J. Baudon, M. Hamamda, G. Dutier, V. Bocvarski, M. Boustimi, F. Perales, and M. Ducloy, Adv. OptoElectron. **2012**, 734306 (2012).
[18] M. Hamamda, F. Perales, G. Dutier, C. Mainos, J. Baudon, M. Boustimi, and M. Ducloy, Eur. Phys. J. D **61**, 321 (2011).
[19] R. Mathevet, K. Brodsky, B. J. Lawson-Daku, C. Miniatura, J. Robert, and J. Baudon, Phys. Rev. A **56**, 2954 (1997).
[20] C. Cohen, B. Diu, and F. Laloë, *Mécanique Quantique* (Hermann, Paris, 1973).
[21] C. Cohen, J. Dupont-Roc, and G. Grynberg, *Photons and Atoms* (Wiley, New York, 1989).
[22] M. Boiron and M. Lombardi, J. Chem. Phys. **108**, 3431 (1998).
[23] Y. Goldfarb, J. Schiff, and D. J. Tannor, J. Chem. Phys. **128**, 164114 (2008).
[24] E. J. Heller, J. Chem. Phys. **62**, 1544 (1975).
[25] M. Hamamda, M. Boustimi, F. Correia, J. Baudon, T. Taillandier-Loize, G. Dutier, F. Perales, and M. Ducloy, Phys. Rev. A **85**, 023417 (2012).
[26] Y. Yin, Q. Zhou, L. Deng, Y. Xia, and J. Yin, Opt. Express **17**, 10706 (2009).
[27] R. Fulton, A. I. Bishop, M. N. Shneider, and P. F. Barker, Nat. Phys. **2**, 465 (2006).
[28] R. Fulton, A. I. Bishop, and P. F. Barker, Phys. Rev. Lett. **93**, 243004 (2004).
[29] H. J. Metcalf and P. van der Straten, J. Opt. Soc. Am. B **20**, 887 (2003).
[30] G. W. F. Drake, *Springer Handbook of Atomic, Molecular, and Optical Physics* (Springer, Berlin, 2006).
[31] O. Morsch and M. Oberthaler, Rev. Mod. Phys. **78**, 179 (2006).
[32] T. Lauber, P. Massignan, G. Birkl, and A. Sanpera, J. Phys. B: At., Mol. Opt. Phys. **44**, 065301 (2011).
[33] T. I. Banks and C. M. Bender, J. Math. Phys. **13**, 1320 (1972).